

TESTING AND LESSONS LEARNT OF LISA GPRM

Andreas Neukom⁽¹⁾, Romeo Romano⁽²⁾, Philipp M. Nellen⁽³⁾

RUAG Schweiz AG, RUAG Aerospace, Widenholzstrasse 1, CH-8304 Wallisellen
Emails: ⁽¹⁾andreas.neukom@ruag.com; ⁽²⁾romeo.romano@ruag.com; ⁽³⁾philipp.nellen@ruag.com

ABSTRACT

The Caging Mechanism (CM) is one of the core devices of the LISA Technology Package (LTP) to be flown on the LISA Pathfinder Mission, a technology demonstrator for the LISA mission. As part of the Inertial Sensor System it shall cage and constrain a Test Mass (TM) during launch and subsequently release it within an Electrode Housing (EH) ready to be controlled and measured via electrostatic forces and an interferometer using a Drag Free Actuation and Control System, when the TM is placed in a perfect free-fall or Geodesic Orbit. The two main functions of the CM are to cage the TM during launch which is done by a mechanism called CMSS (Caging Mechanism Sub-System) and to release it into zero-g condition which is performed by the GPRM (Grabbing, Positioning and Release Mechanism), a piezo actuated walking mechanism which has been presented at the ESMATS 2007.

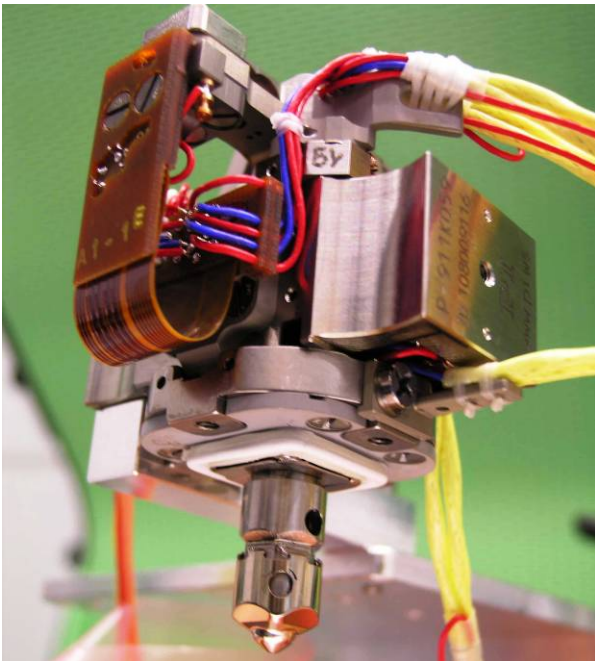


Figure 1: LISA GPRM flight model

A number of unexpected challenging issues revealed during testing. Testing activities, design recovery solutions and lessons learnt of the GPRM are described in detail within this paper.

1. DESIGN OVERVIEW

1.1. Caging Mechanism

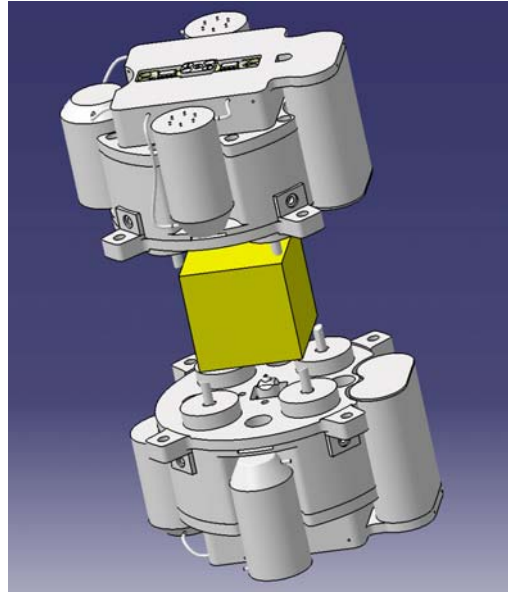


Figure 2: Caging mechanism

The GPRM is part of the CM which itself consists of two parts, one (+z) located above the TM and one (-z) located below the TM. Each part of the CM contains two separate and independent mechanisms. The CMSS (one at +z and one at -z) cages the TM at its 8 corners with fingers during launch as well as during on ground operation and storage. The loading system of the CMSS is a hydraulic system where 4 actuators apply the preload to the TM by the 4 fingers. Once in the final orbit the CMSS releases the preload and hands over the TM to the grabbing fingers of the upper and lower GPRM. Now the GPRM has to position the TM with a high accuracy and release it into zero-g condition within the cavity of the electrode housing which is a few mm larger than the TM. Should the TM be out of control of the forces of the electrostatic suspension system the GPRM grabs the TM again, positions and releases it again.

1.2. Key Requirements

Following key requirements are defined for the CM:

Table 1: Key requirements for caging mechanism

Requirement	Value
No damage to the constrained TM (especially gold surfaces)	
TM linear release velocity	< 5 $\mu\text{m}/\text{sec}$
TM angular release velocity	< 100 $\mu\text{rad}/\text{sec}$
TM linear position accuracy	< 60 μm in all axes
TM angular position accuracy	< 60 μrad about 2 axes
Quasi static design load	± 75 g for all axis
Random loads	~ 25 g_{rms} in all axes
Static launch acceleration (superposed to random loads)	10 g
Tiny envelope for the CM	$\phi 125 \times 65$ per CM half
Knowledge of TM position	< 5 μm over 2 mm range
Grab TM from all possible position	
Gold coated constraining elements and gold coated TM	
No use of magnets nor ferromagnetic materials	
Extremely high out-gassing and cleanliness requirements	

From Table 1 it is obvious that not only the accuracy requirements are challenging but also unusual requirements using two gold coated, separable I/F surfaces, high preloads at launch for the CMSS and no use of ferromagnetic materials.

1.3. GPRM Design

The GPRM consists of 2 main sub-assemblies:

- Actuator unit with the Nexline walking mode piezo actuator and all none moving items

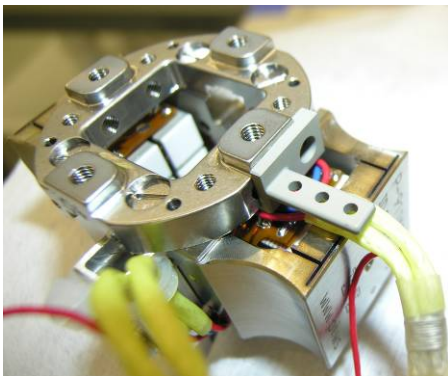


Figure 3: Actuator unit

- Grabbing finger unit (GF) containing all elements that are moving

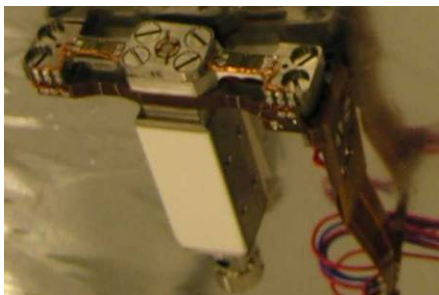


Figure 4: Grabbing finger unit

Within the GF the preloaded release tip and 2 piezo stack actuators are housed. The stack actuator retracts the release pin very fast which induces an inertial release of the TM.

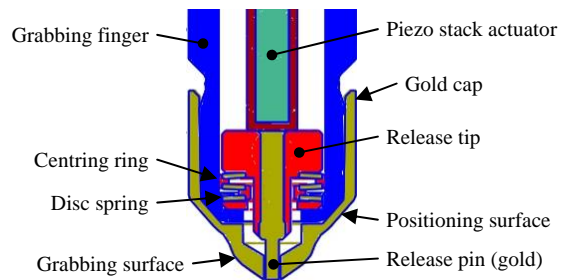


Figure 5: Inner parts of grabbing finger

The GF is preloaded by the Nexline and guided in the lateral direction by a spring preloaded side guiding system consisting of sliders on the fix and rollers on the flexure side.

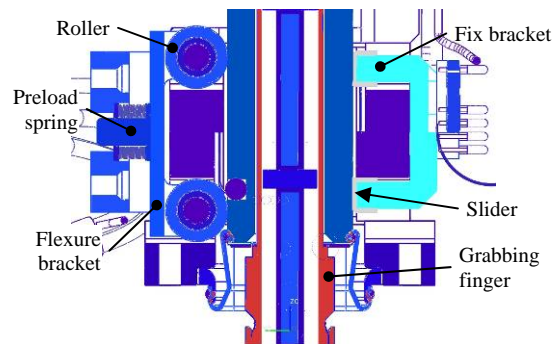


Figure 6: Side guiding system

Built-in force and position sensors measure the interface force to the TM and its absolute position.

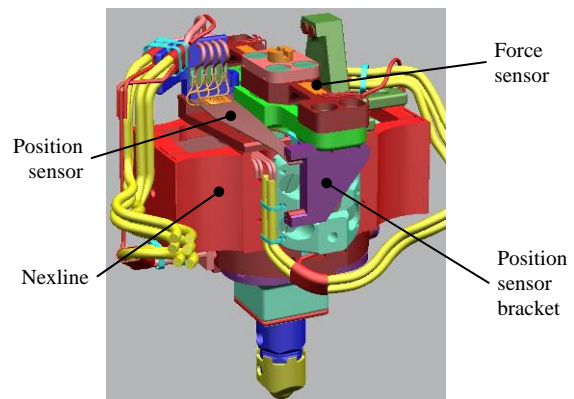


Figure 7: Location of force and position sensor

1.4. GPRM Functional Description

The TM is grabbed and positioned by the GF of 2 GPRMs located on +z and -z side of the TM.

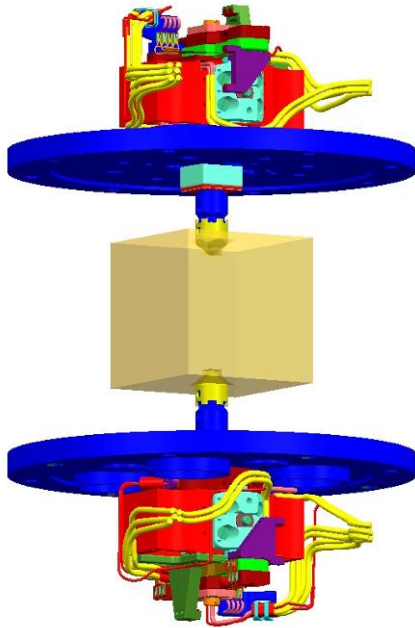


Figure 8: Location of GPRMs in CMA

The functional steps of the GPRM are shown in Figure 9:

- The completion of the grabbing sequence is indicated by a sudden increase of the force signal
- During the pass-over phase from the GF to the release pin the stack actuator is continuously powered while at the same time the Nexline steps backwards such that the total force remains constant.
- After this pass-over phase the TM is released within less than 1 msec by a simultaneous retraction of the release pins.

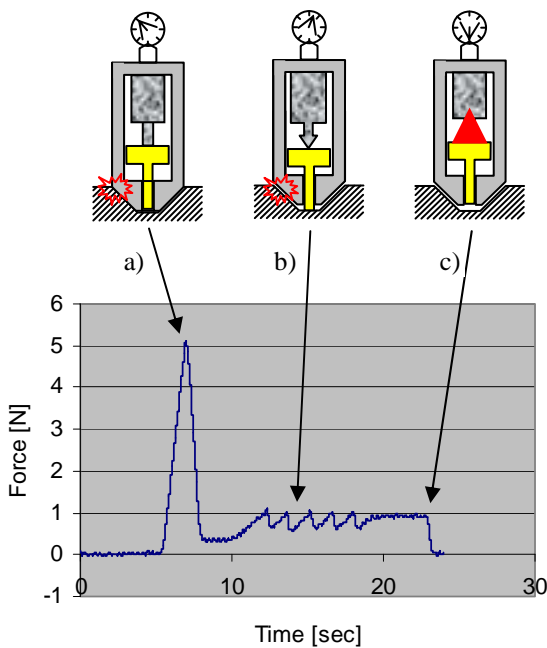


Figure 9: Hand over and release sequence

2. DETECTED DESIGN ISSUES

2.1. Nexline Holding Force Capacity

The GF is held by the Nexline piezo elements via frictional forces. Applying forces over the holding capacity causes the GF to slide.

The inertia forces of the GF during launch are much smaller than the holding capacity of the Nexline. Consequently the vibration test in movement direction passed without problems. However during the vibration test in lateral direction the GF moved in vertical direction.

The initial cause of this movement is a displaced centre of gravity with respect to the frictional area between the GF and the Nexline feet. Due to this offset the GF rotates when excessive lateral forces are applied. Once sliding a continuous movement in direction of the average force vector occurs which during the test was the gravity direction.

Safety considerations led to the definition of a new requirement which asks to superpose a static launch acceleration of 10 g to the vibration environment. Under this combined loading the grabbing finger shall not move.

The corresponding design solution is the implementation of a launch lock, which consists of a pin in the GF. This pin acts as a geometrical obstacle for one of the preloaded rollers of the side guiding system.

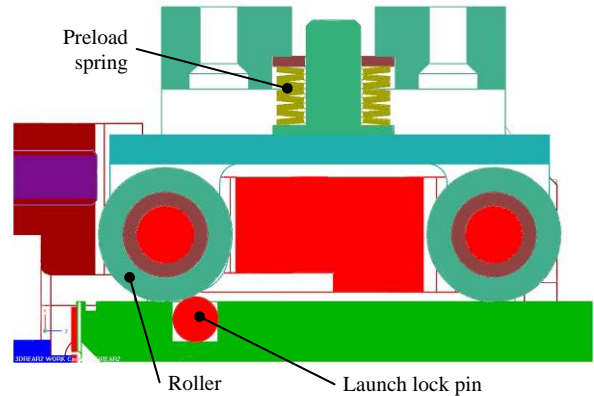


Figure 10: Launch lock consisting of pin and roller

The force profile when travelling over the launch lock was analysed and verified by test. The analytical model fits well with the measured values.

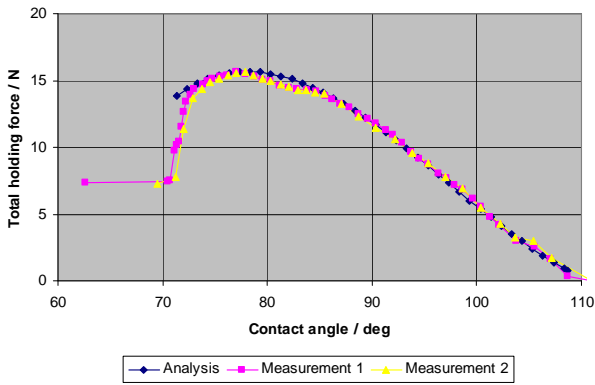


Figure 11: Holding force profile of launch lock

The implementation of the launch lock assures that the grabbing finger stays in place during launch. On the other hand the additional holding force acts as a resistive load on the Nexline during operation in orbit, leading to a reduced motorisation factor which is a new issue that has to be solved (refer to section 2.4).

Lessons learnt:

- Parts can move perpendicular to the vibration loads.
- Load cases can not be split in different axis when forces are transferred by friction.
- Check if static launch accelerations and random loads have to be superposed.
- Carefully check that corrective actions do not induce new problems.

2.2. Hysteresis of Position Sensor

During position sensor calibration on the QM a considerable hysteresis was recorded whereas on the engineering models no such phenomenon was noticed.

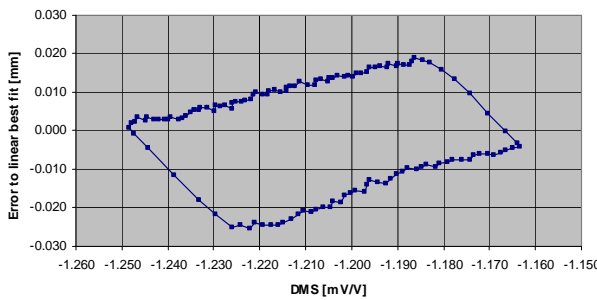


Figure 12: Measured hysteresis of position sensor

Most of the hysteresis is related to a rotation of the grabbing finger. Since the position sensor contact point is laterally displaced with respect to the movement axis a rotation of the grabbing finger influences the position sensor signal. Tests with an autocollimator confirmed that a kick of the tilt angle occurs when the movement of the grabbing finger is reversed.

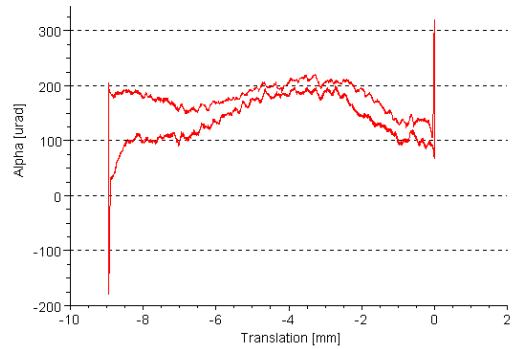


Figure 13: Angular position of grabbing finger

Two main causes were found for the rotation:

- Side forces and torques are internally generated by the Nexline since the deformations of the Nexline shear piezo elements are subject to variations.
- Friction forces between the side guiding and the GF are different on the flexure and the fix side guiding which induces a torque on the GF.

The criticality of the side kick is twofold:

- The angular position of the TM is changed
- The small gaps between the GFs and the TM are further reduced so that a risk exists that the GF retouches the TM during the pass-over process.

A geometrical analysis of the grabbing process shows that during the pass-over of the first GPRM the gap between the grabbing finger and the TM grows up to 4 μm and reduces during the pass-over of the second GPRM due to the tilt kick to 2 μm .

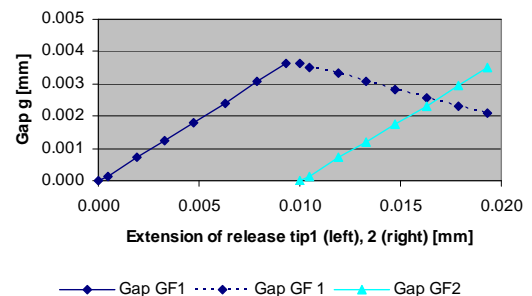


Figure 14: Gap between TM and grabbing finger

The analysis demonstrates that the GF does not retouch the TM during release under worst case conditions. Nevertheless the side guiding preload was increased from 40 to 55 N which reduces the tilt kick of the GF and increases the gap between the TM and the GF.

Lessons learnt:

- Sensor inaccuracies are not always caused by the sensor.
- Sliding elements in a high precision mechanism can induce severe inaccuracies due to tribological effects.

2.3. Unstable Position Sensor Signal

The position sensor consists of a deflectable Titanium blade where on the upper and lower side resistance strain gauges are applied and wired in a full Wheatstone-bridge.



Figure 15: Position sensor

During calibration activities at different temperatures unexpected results were obtained that could not be correlated with the temperature. Three effects have been identified as main cause:

- Test harness
- Creep
- Humidity

The GPRM is delivered with flying leads of excessive length. Resistances of flight hardware and test wires and connectors influence the read-out of the sensor signal. A final calibration can therefore only be done after full integration of the GPRM into the CM.

Creep is an intrinsic characteristic of strain gauges. It consists of a metallic component related to the electrical grid and a plastic component related to the support material. According supplier information the overall creep can at least partially be compensated.

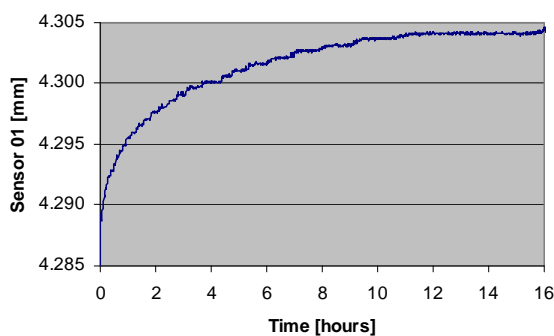


Figure 16: Drift of position sensor signal

The position sensor is also needed during integration of the GPRM into the CM. It has not only to operate in vacuum but also in ambient condition and under dry Nitrogen (for measurements at low temperature). Figure 17 shows sensor signals at the same geometrical position but in different environments.

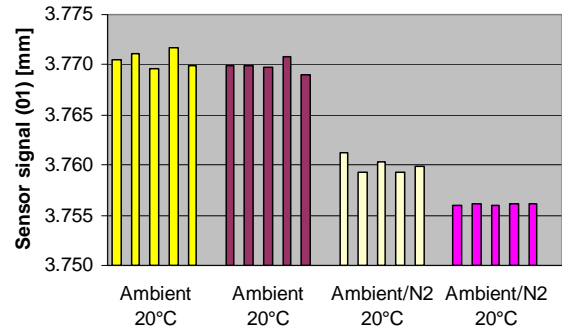


Figure 17: Position sensor signal in different environments

Lessons learnt:

- The influence of test harness on sensor signals has to be considered and compensated.
- Strain gauges should be coated for accurate and consistent measurements in different environments and to protect them from being damaged.

2.4. Low Motorisation Factor

During QM testing a low motorisation factor of the GPRM was measured in air despite a thorough analysis. Since the sliders and the roller sleeves of the side guiding system are made out of Vespel SP3 (containing MoS₂) a high friction coefficient due to humidity was identified as cause. After storage in vacuum the motorisation has recovered "as expected".

Also on the FM a low motorisation factor was measured which however did not recover after vacuum exposure. Detailed investigations were performed and all contributors to the motorisation factor were assessed and separately tested.

- Nexline performance: The actuation force of the Nexline has been measured without any side guiding system. The test showed that the Nexline works properly without any loss of performance.
- Motorisation analysis: A motorisation analysis according ECSS showed that during travelling over the launch lock the allowable friction coefficients in the side guiding system must not be larger than 0.06. Even with such low friction coefficient the frictional part is 2/3 of all resistive forces.
- Friction between side guiding and linear runner: Friction forces between the original sliders / roller sleeves (made out Vespel SP3) and the linear runner (made out of Titanium) were measured at ambient and vacuum conditions.

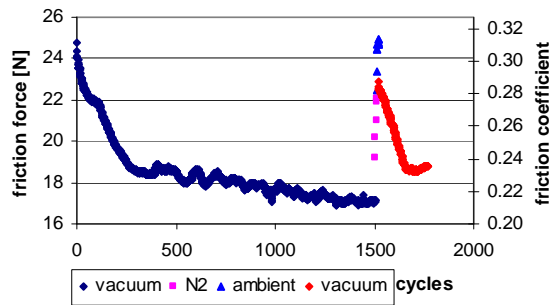


Figure 18: Friction coefficient of Vespel SP3

After a run-in phase in vacuum the friction coefficient establishes at approximately 0.22. Purging first with Nitrogen and then with air increases the friction coefficient within a few number of cycles to the initial value of 0.31. After 100 cycles in vacuum the friction coefficient almost reaches the value after the run-in.

According supplier data sheet and other sources the friction coefficient in vacuum should be less than 0.04.

Since the measured friction coefficient is far above the maximum required value of 0.06 alternative materials for the side guiding system were investigated. It was found that only pure PTFE can reach the required value since low friction requires low speed and low pressure loads. With an effective speed of 0.1 mm/sec and an effective pressure of 1.5 MPa these conditions are clearly fulfilled.

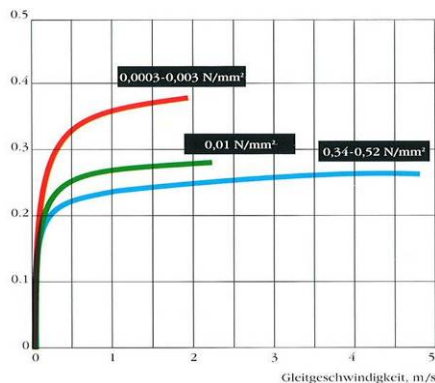


Figure 19: Influence of speed on PTFE friction

For the sliders the maximum pressure stress is within tolerable limits but it is exceeded for the roller sleeve. Hence a metallic bushing coated with PTFE has to be used instead of pure PTFE.

The friction test was repeated with PTFE sliders. After a run-in of about 100 cycles a friction coefficient of less than 0.05 is reached. In contrast to Vespel SP3 it does not increase when operated in air.

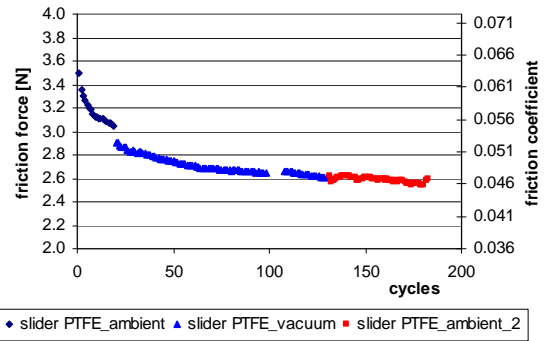


Figure 20: Friction coefficient of PTFE sliders

An additional friction test between PTFE coated bushings (Glycodur bearing) and a Titanium shaft was performed. Initially the friction coefficient is 0.05 and becomes after only a few run-in cycles 0.04 which even slightly decreases in ambient conditions.

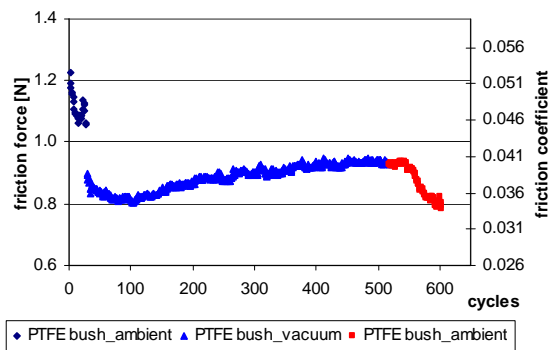


Figure 21: Friction coefficient of PTFE coated bushings

The results of the friction tests are shown in Figure 22. Changing the material for the side guiding sliders and rollers from Vespel SP3 to PTFE leads to a ECSS compliant motorisation factor.

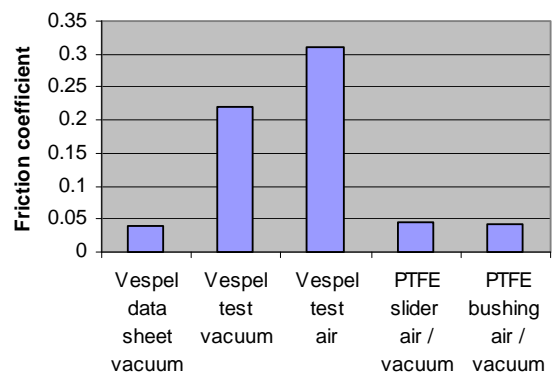


Figure 22: Comparison of friction coefficients

Lessons learnt:

- Never rely on friction coefficients provided by suppliers or tested for other applications.

- Investigate cause of NCR on QM in detail and do not rely on common knowledge. Recovery of motorisation factor on QM was by chance.
- Do not use humidity sensitive material when operation in ambient and vacuum conditions is required.

2.5. Gold Coating

The specified gold coating on the TM and the GF has severe drawbacks:

- Low strength leading to surface damages and hence disturbing the electrical field inside the EH

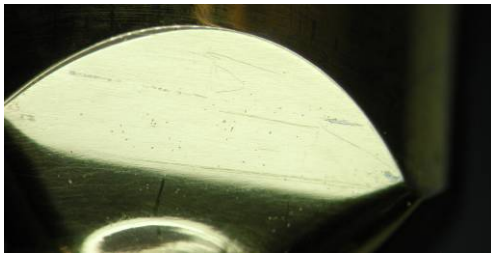


Figure 23: Defects of gold coating

- High friction coefficient which prevents the GF to fully engage into the TM which results in an inaccurate positioning and may even prevent a successful pass-over process so that no release can be done
- High adhesion forces which could lead to excessive high residual speed after release of the TM

The GF was originally made out of Titanium and its tip was gold coated. This design was changed by fixing a cap made out Platinum-gold to the front part of the GF. The caps were cast by a dental technician who also tried several fixations to the Titanium base material such as welding, glueing and riveting which all did not work. At the end a goldsmith found the correct method which was border crimping.

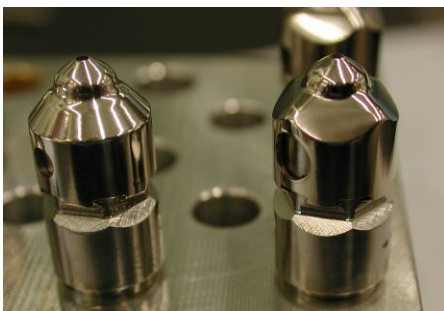


Figure 24: Platinum-gold caps on Titanium GF

Lessons learnt:

- Insist to replace requirements that can technically not be fulfilled.
- Think outside the box to find new solutions (as in this case dental technician and goldsmith)

3. AIT ISSUES

3.1. Cleanliness

The stringent cleanliness and outgassing requirements defined for the CM lead to a number of difficulties for the GPRM development.

- Coating of the strain gauges and their very thin wires is not possible. Since the harness is very fragile there is a considerable risk that during integration, handling and testing damages could occur.
- At start of the project it was stated that the Nexline does neither create wear nor debris. Run-in and life cycle testing showed the contrary (see debris particles in Figure 25).

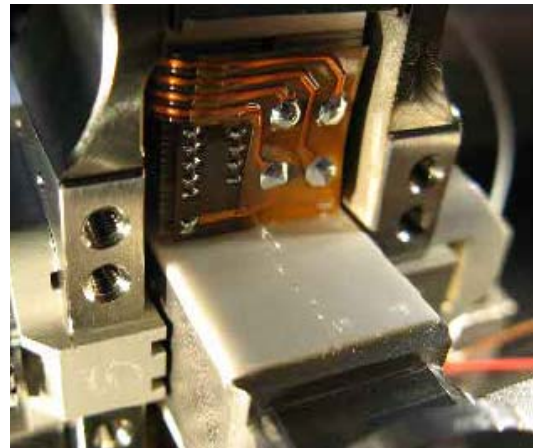


Figure 25: Wear particles generated by Nexline

- To prevent any ingress of the particles into the EH a dust trap has been implemented. It consists of an extruded PTFE hose, one end fixed to the actuator bracket (which does not move) and the other end fixed to the linear runner.



Figure 26: Dust trap membrane

- An additional effect observed was that after cleaning of coaxial wires in IPA the isolation properties are lost. However they can be restored by a bake-out at 100°C over at least 2 hours without performance degradation.

Lessons learnt:

- Verify supplier information of novel devices by own tests or attend tests at supplier site
- Cleaning can change material (isolation) properties

3.2. Assembly and Integration

The GPRM is very small and has a number of very sensitive components. This makes assembly and integration extremely difficult and time consuming.

- **Glueing**
Application of glue in the correct amount and at the correct place is quite difficult for small mechanisms. It poses the risk that glue ingresses into gaps which can end up in a complete loss of the mechanism or parts of it.
- **Welding**
Due to volume limitations the force sensor is laser welded to the GF without any possibility for disassembly. Since the GF are not exchangeable between the Nexlines a defective force sensor makes the whole mechanism unusable.
- **Harness and Soldering**
The small wires are fragile and the mass of flying leads can be sufficient to damage the harness. To prevent this temporary fixation jigs are needed. Final harness fixation is extremely important, difficult and time consuming.
Soldering becomes a real issue since access is quite often limited and the solder points are very small.

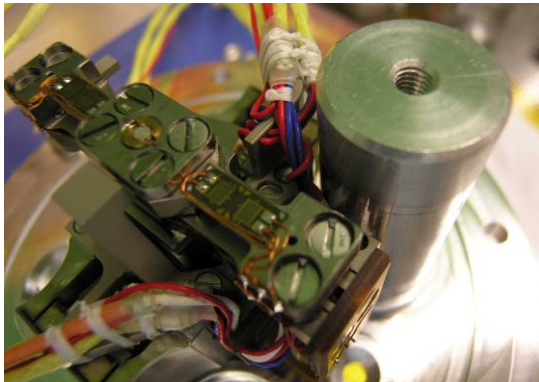


Figure 27: Limited access

This makes also solder inspection difficult. The tendency to extremely magnify the solder points for inspection can lead into an impasse. Using SEM photos as shown in Figure 28 makes it difficult to assess the quality of a solder connection according to ECSS rules since it is not known which defects are normal and which ones pose really a problem.

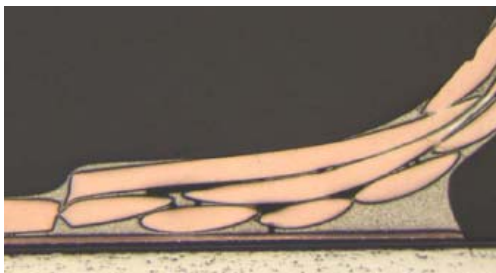


Figure 28: SEM photo

Lessons learnt:

- Design for disassembly
- Assembly and integration of small mechanisms is difficult and very time consuming
- Provide sufficient spare parts for training of activities (soldering, integration)
- Define dedicated person for soldering, assembly and integration activities and allow for sufficient training
- Consider much more time for these activities than one normally would estimate.

3.3. Testing

For small high precision mechanisms the accuracy of the measurement equipment and the influence of other test equipment becomes a limiting factor.

- With a 3D measurement machine very accurate measurements in the micrometer range can be done. In most cases this is sufficient accurate for geometry and position measurements. However it can lead to considerable inaccuracies if angles are calculated based on such measurements. Assuming a machine accuracy of $\pm 1 \mu\text{m}$ and a base length of 2 mm results in an angular uncertainty of $\pm 500 \mu\text{rad}$ which is already out of specification for the GPRM.
- Small changes in the cleanroom conditions may induce errors in the test equipment which jeopardise the goal of the measurement. Beside the accuracy of the test equipment itself also test harness (wire length and size) and connectors have to be considered.

Lessons learnt:

- Use adequate large distances for evaluation of angles or perform tests with autocollimator
- Consider the accuracy of the measurement equipment for evaluation of test results.

4. ACKNOWLEDGEMENT

The authors would like to thank all involved persons for their support, especially Paolo Leutenegger and Paolo Radaelli from Thales Alenia Space, Ingo Koeker from EADS Astrium and Hans Rozemeijer from ESA.